Journal of Nuclear Materials 377 (2008) 458–466

Contents lists available at ScienceDirect

Journal of Nuclear Materials

journal homepage: www.elsevier.com/locate/jnucmat

Phase separation of metal-added corium and its effect on a steam explosion

B.T. Min *, J.H. Kim, S.W. Hong, S.H. Hong, I.K. Park, J.H. Song, H.D. Kim

Thermal Hydraulics Safety Research Division, Korea Atomic Energy Research Institute, 150 Dukjin-Dong, Yusong, Taejon 305-353, Republic of Korea

ARTICLE INFO

Article history:
Received 4 October 2007
Accepted 8 March 2008

ABSTRACT

To simulate a relocation of molten core material and its interaction phenomenon with water during a severe accident in a nuclear reactor, a typical corium of $UO_2/ZrO_2/Zr$/Stainless steel mixed at a 62 wt%, 15 wt%, 12 wt% and 11 wt%, respectively, was melted and then cooled down to become a solidified ingot. It was shown that the molten corium was separated into two layers, of which the upper layer was oxide mixtures and the lower layer was metal alloys. The upper layer was UO_2 and ZrO_2 and the lower layer mostly consisted of metal mixtures such as uranium, zirconium and stainless steel. Iron content varied with the positions and about a half of it existed as an alloy such as Fe_2U. Uranium metal was produced by reduction of UO_2 by zirconium metal. The average densities of the upper oxide layer and the lower metal layer were 8.802 and 9.411 g/cm^3, respectively. In another test, metal-added molten corium was poured into water and it showed that a steam explosion could occur by applying an external trigger.

1. Introduction

In a nuclear reactor, a hypothetical severe accident could be considered during transients such as a loss-of-coolant accident, a steam generator tube rupture, an anticipated transient without a scram, and a station blackout. Although the reactor would scram by those transients, the uncovered cladding material, UO_2 fuels and internal structures could be melted by the decay heat generation from the fuel during those accidents. Molten core material, the so-called corium, would be relocated and settled on the bottom head of the reactor pressure vessel (RPV). Molten corium could attack and finally melt the RPV.

Though the severe accident at Three Mile Island Unit 2 (TMI-2) had melted about 50% of the core materials and about 20% of them were relocated into the bottom of the RPV, a RPV failure did not occur [1,2]. The reason was that a small amount of water was continuously supplied and a sufficient amount of water was introduced at 16 h after the accident. However, the melt-through of the RPV could be considered to depend on the molten corium composition, its temperature and the accident scenario. One of the most probable reasons for a RPV failure is the corium composition. The reactor pressure vessel could be damaged by metals in the corium, which has a higher thermal conductivity when compared with oxides. Therefore, the molten corium component containing metals is very important from the viewpoint of an in-vessel-retention (IVR).

In this study, a prototypic metal-added corium simulant was used for the tests. UO_2 pellets, zirconia, zirconium metal and stainless steel were charged in a cold crucible, and melted with a high frequency induction heater. The molten stimulant was cooled down to become a solidified ingot for the measurement of its phase separation. The ingot was sampled and analyzed for its composition by chemical and physical means.

If the RPV is ablated, the molten hot corium pours into the coolant in the cavity which leads to a steam explosion. A steam explosion produces excessive amounts of vapor by an interaction between the hot melt and the surrounding cold and volatile water, in which the melt rapidly releases its thermal energy into the water when they come into direct contact. This physical process may be a hazard to the RPV structure and the containment due to this energetic event, in the form of a dynamic pressurization from a shock wave interaction with the structural walls. To study this event, there experiments have been performed with core simulant materials such as FARO [3,4] and KROTOS [5,6], but they revealed a weak steam explosion or no explosions. Recent MASCA tests have revealed a layer inversion, i.e. metal below oxide, due to a heavy metal (uranium) extraction from UO_2 by cladding and structural metal components (Zr and Fe) [7].

In this study, the metal-added corium was melted and solidified to investigate its phase separation or the melt was delivered into the water coolant to study the steam explosion phenomenon. If the metals are separated from the oxides before delivery into water, the metal part may cause a steam explosion easily. But, if the molten oxides are mixed evenly with the metals it would be difficult for a steam explosion to occur. Since the oxides including metals will be mixed well by the electromagnetic force in the cold crucible [8], its effect on the steam explosion was tested.

* Corresponding author. Tel.: +82 42 868 8722; fax: +82 42 863 3689.
E-mail addresses: btmin@kaeri.re.kr (B.T. Min), kimjh@kaeri.re.kr (J.H. Kim), swhong@kaeri.re.kr (S.W. Hong), hsh4004@kaeri.re.kr (S.H. Hong), gosu@kaeri.re.kr (I.K. Park), dosa@kaeri.re.kr (J.H. Song), hdkim@kaeri.re.kr (H.D. Kim).

0022-3115/$ - see front matter © 2008 Elsevier B.V. All rights reserved.
doi:10.1016/j.jnucmat.2008.03.019

2. Experimental facilities

A series of tests were performed by using metal-added corium as a melt. The purposes were to confirm the phase separation possibility and the effect of metal-added molten corium on a steam explosion. These tests provided us with some information on the effect of a metal-added corium on a RPV erosion and on a steam explosion. These tests were performed in the test for real corium interaction with water (TROI) facility, in which the corium is melted in the upper furnace vessel and interacts with the water in the lower pressure vessel. The upper and lower vessels are designed to sustain 3.0 MPa at 212 °C against a static load.

For the melting tests, induction heating in a cold crucible was used as a melting technique [9,10]. Though a cylindrical cold crucible is in contact with a high temperature melt during induction heating, it maintains several tens of °C because of cooling with circulating water in the double copper tube-fingers. The crust of the charged material forming between the melt and tube fingers (refer to Figs. 1 and 4) serves as a crucible.

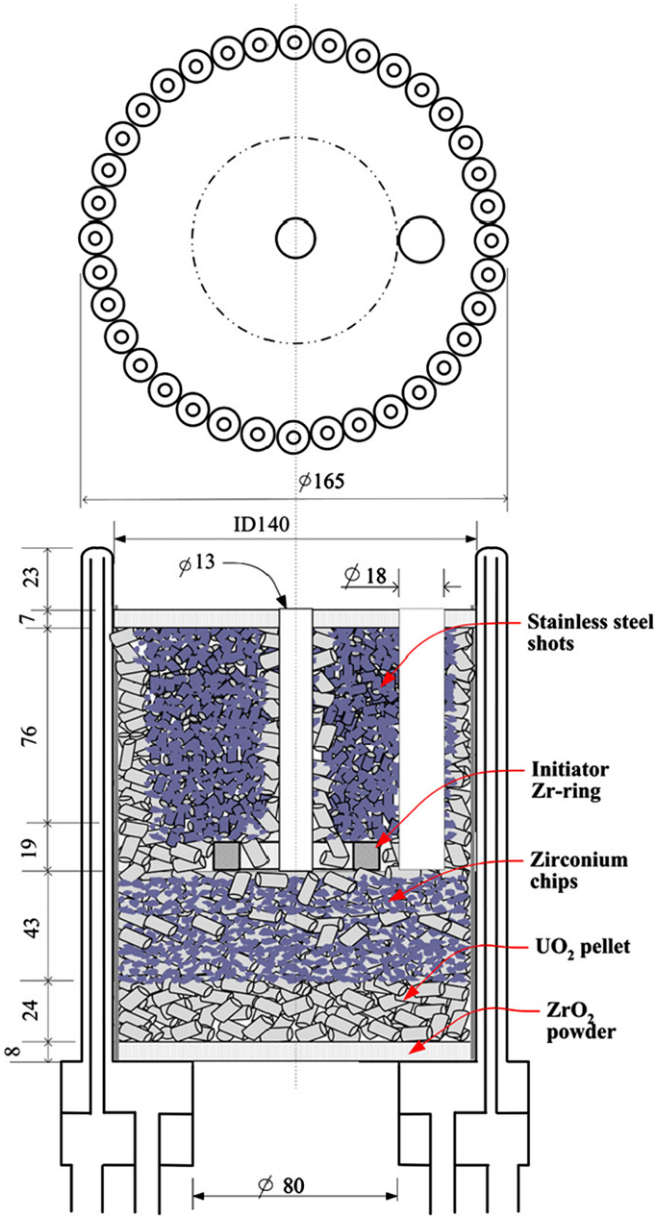

Fig. 1. Schematic diagram of the typical charging pattern in the cold crucible for the TROI-49 test.

The crucible inner diameter was 14 cm and its height was 20 cm. The induction heater had a maximum power of 150 kW and a frequency of 50 kHz. The inner diameter of the induction coil surrounding the outside of the crucible was 21.5 cm, the height was 18 cm and the number of coil turns was 12. The molten corium was solidified for a layer separation test or it was delivered to the water through a delivery hole for a corium–water interaction test. The delivery hole was blocked with a plug (8 cm in diameter) during melting.

3. Experimental results

3.1. Procedures

TROI-49 and 50 were performed for a phase separation, and TROI-51 was performed for a fuel coolant interaction (FCI) by using metal-added corium. The typical charging pattern is shown in Fig. 1 for TROI-49. The gap between the fingers of the cold crucible wall was coated with wet ZrO_2 powder and dried for hours in order to protect the fingers. The thickness of the ZrO_2 coating was 0.5–0.8 mm, and the mass was 0.75 kg. The thickness of the zirconia bottom liner was 8 mm. The UO_2 pellets filled the bottom and circumference of the crucible to protect the fingers from an attack of the hot molten metals with a relatively lower melting temperature. The upper part was filled with stainless steel and zirconium metal chips, and covered with a small amount of zirconia.

The initiator made of a Zr-metal ring, which enabled the charged mixture to be melted at an initial stage, was installed at 7.5 cm above the inner bottom of the crucible. Its inner diameter was 5 cm, its outer diameter was 7 cm, its height was 1.5 cm, and its weight was 0.104 kg.

The charged composition of TROI-49 was 62.25%, 15.0%, 11.70% and 11.05% at a weight percent of UO_2:ZrO_2:Zr:SS including the ZrO_2 coating of 0.75 kg (UO_2:ZrO_2 := 80.6:19.4), and the total charged mass was 15.96 kg. This zirconium weight included the weight of the zirconium metal initiator. The average charge density was 5.858 g/cm^3.

TROI-50 was charged with 59.53%, 18.02%, 11.90% and 10.56% of UO_2, ZrO_2, Zr and SS including the ZrO_2 coating of 0.75 kg and its total charged mass was 14.456 kg. This composition was very similar to that used in the OECD/MASCA program [7]. The average charge density was 5.833 g/cm^3.

The melt temperature in the cold crucible was measured by an optical two-color pyrometer (IRCON 3R-35C15) installed at the top of the furnace vessel. Since the temperature was measured through a 13 mm hole at the center of the charged material, as shown in Fig. 1, the surface temperature of the melt was measured. However, the measured temperature would be similar to that of the inside of the molten material, because the melt was mixed well by an electromagnetic force [8,11]. In addition, a vent hole of 18 mm in diameter was provided between the center and the inner wall of the crucible to vent the gases and aerosols generated during the melting stage.

The furnace vessel containing the charged cold crucible was purged with argon gas for 40 min before induction heating and the argon gas was continuously supplied at a very slow flow rate into the furnace vessel during the heating to prevent a rapid oxidation of the zirconium metal chips which could cause a melt eruption.

After the charge was sufficiently melted, the argon gas supply from the lower inlet of the furnace vessel was stopped, and afterwards the gas was blown through a gas supply system above a hole of the charged material. This system enabled us to measure the melt temperature more accurately by removing the aerosols gener-

ated during the melting. Though the argon gas supplied to the top of the charged material, the measured temperature was still unstable owing to the generation of many aerosols through the hole. As shown in Fig. 2, the pyrometer began to display its lower measuring limit temperature of 1773 K from 500 s after the initiation of the heating in accordance with the absorbed power. The melt temperature was maintained constant at about 2730 K even though the power input was increased as shown in Fig. 2 for TROI-49.

3.2. Phase separation test

3.2.1. Ingot separation and results

After the melting of the metal-added corium, the melt was left to cool down by supplying cooling water into the cold crucible. Thereafter, the cold crucible was dismantled to observe the solidified ingot after a removal of the top liner part in a ventilated hood. The top liner part of the cold crucible was crushed and it was shown to be partially melted. A photograph in Fig. 3 shows that the lower surface was dark in color with hive-type pores and contained unmelted UO_2 pellets, zirconium metal and stainless steel shots (Fig. 3(a)). Since the top liner part was partially melted, its components were different depending on the location.

The TROI-49 and 50 tests showed similar phenomenon of an ingot separation, and the solidified corium was easily separated into two parts. The upper part had a dark color (Fig. 3(b)) and the lower part had a metallic shine (Fig. 3(c)). The melt might be separated into two layers by a density difference during cooling.

For TROI-49, the molten material surface settled 91 mm below the surface of the top liner, as shown in Fig. 3. The solidified ingot height was about 55 mm and 31 mm for the upper and lower parts, respectively. The mass of the unmelted top liner, upper lump and lower lump was 5.075 kg (32.43%), 8.21 kg (52.46%) and 2.365 kg (15.11%), respectively. The total mass of the products was 15.65 kg and the mass of the solidified ingot was 10.575 kg. Here, the collected aerosols in the vent gas in the cyclone (0.36 g) were ignored. Since the total charged mass was 15.961 kg and the loss was 0.311 kg, the masses of the charged materials and products were almost balanced.

For TROI-50, the height of the upper and lower ingot was 91–105 mm depending on the position as shown in Fig. 4. The outside of the ingot was composed of a side crust of 3–5 mm in thickness. The masses of the upper and lower ingot were 8.06 kg and 3.56 kg, respectively.

3.2.2. Physical and chemical analysis

The solidified corium ingot was sampled and analyzed by inductively coupled plasma-atomic emission spectrometry (ICP-AES), electron probe micro analyzer (EPMA), X-ray diffraction (XRD) and a density measurement. The lower part of the ingot had a metallic shine, because it was glittered as a lighter flint due to a little friction with other metals, and it showed the characteristics of metallic uranium and zirconium.

3.2.2.1. ICP-AES analysis. Since the upper layer of the ingot had a larger mass compared to the lower layer as shown in Figs. 3 and 4, the upper layer was sampled at two places and the lower was sampled at one place. As shown in Table 1, the total mass of all the elements in the solidified upper layer is about 78–85% and that of the lower layer is about 95%. The reason is that ICP-AES dissolves a sample and analyzes the cations like metals, but not oxygen, and that the upper layer consists of oxides and the lower layer mainly consists of metal. Next, the contents of the chemical compound in the upper part were calculated under the assumption that the produced ingot consisted of oxide compounds, and the results are shown in Table 2. The sum of the calculated compounds as oxides for the upper layer is almost 100% for TROI-49 and about 95% for TROI-50. Therefore, the upper layer could be considered as oxide compounds. For TROI-50, the reason why the sum was as low as 95% was inferred to be due to a sampling problem accompanied by a low miscibility of iron, to be reviewed later. If the lower layer was calculated by assuming it to be oxide compounds, their amounts exceeded 120%. So it is expected to exist in a metal state. The average uranium oxide content of the upper layer was about 70% for the two samples of TROI-49 and 62.5% for TROI-50 as shown in Table 2.

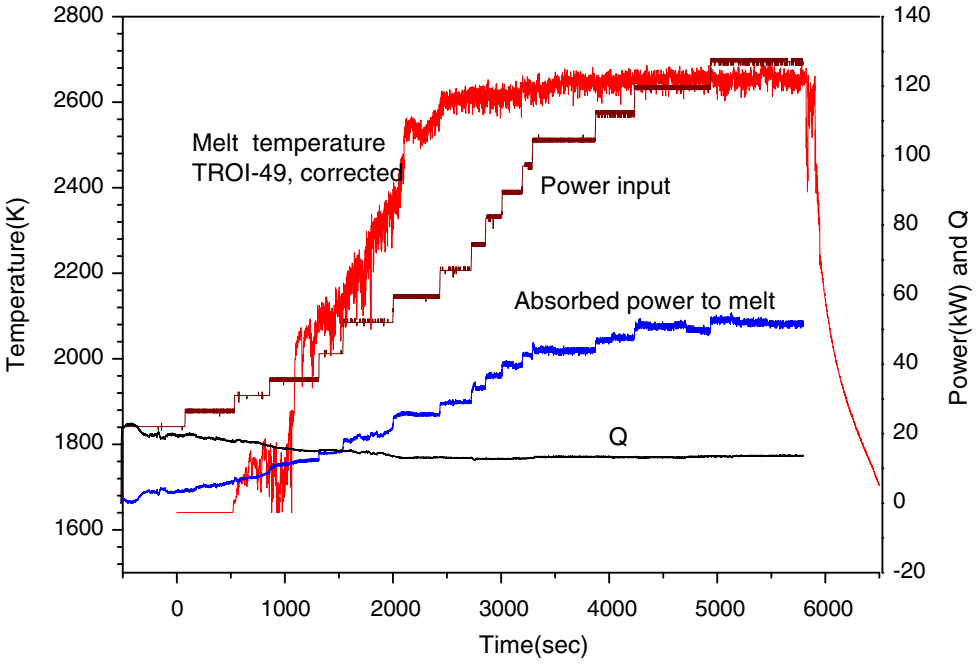

Fig. 2. Melt temperature and the melting performance curves in TROI-49.

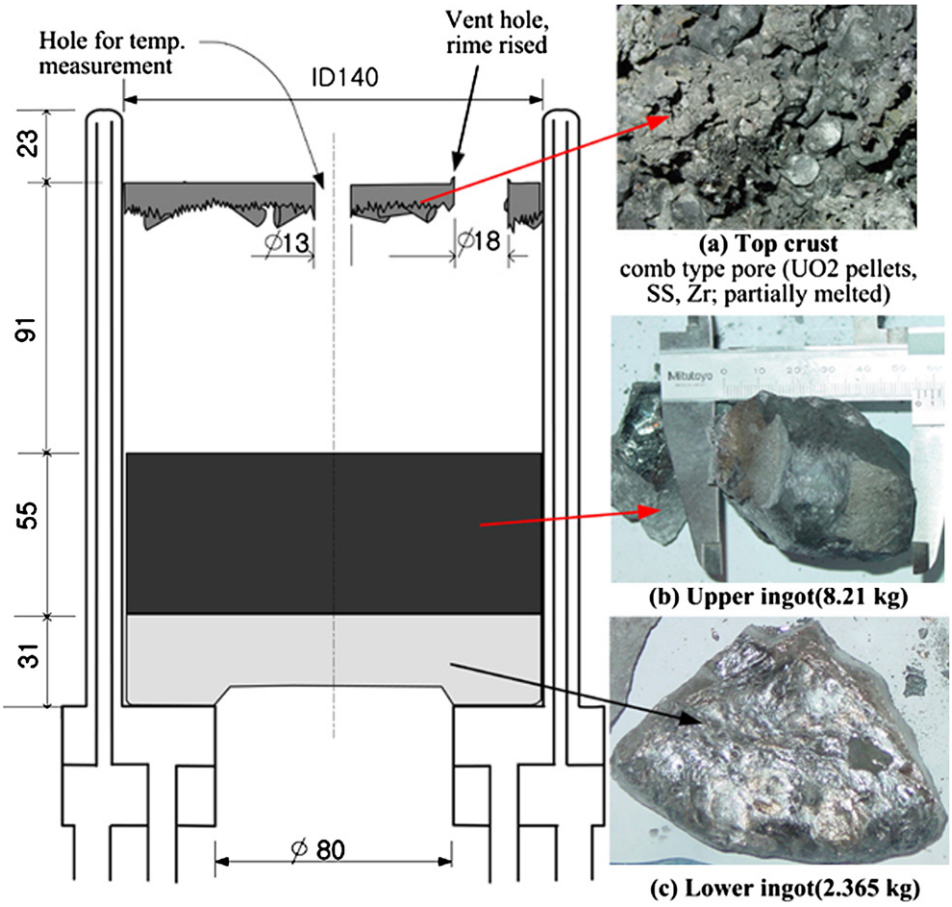

Fig. 3. Sketch and photos of the solidified corium in the cold crucible (TROI-49).

3.2.2.2. EPMA analysis. To review the homogeneity of an ingot, three samples of the upper layer were analyzed by EPMA. The analysis deviation for them was lower than ±2%, and so the averaged values for the three points are shown in Table 3. Since the iron contents for the lower layer varied considerably, this will be reviewed in Section 3.2.2.5.

In the EPMA analysis, it is empirically known that analysis of gases like oxygen and light metals such as sodium has large uncertainty. Analysis results are shown by relative fractions of the selected target elements and the sum for those elements is expressed as 100%. So, we made a recalculation on the results shown in Table 3: oxygen was excluded, relative fractions of metal elements were obtained, oxides and metals were assumed for the upper and lower layers, respectively, and mass fractions of components were recalculated. Table 4 shows the calculated results. The calculated results of ICP-AEC shown in Table 2 for the two upper oxide layers are consistent within about 3% when compared with the EPMA results shown in Table 4 except for the ZrO_2 content for the upper layer of TROI-50. The large difference in the TROI-50 might come from the representative sample by an immiscible iron, because the sum of the converted oxides was as low as 94% as shown in Table 2. From these reviews, it was thought that the upper solidified layer was oxides and the lower layer was metal. So, Tables 2 and 4 could be used for the analysis for the oxide layer and the lower metal layer.

3.2.2.3. Chemical compound state of the upper and lower layers. Argon gas was continuously supplied during melting, but air was also supplied instead of argon gas for about 10 min before a melt delivery. However, it seemed difficult for the air to contact with the melt at this time owing to an intensive venting of the aerosols through the holes on the top crust. Since the melt did not interact with the water and then solidified in the cold crucible, the component variation of the melt during solidification could be ignored, so the changes in the chemical components have been made by chemical reactions during the melting process.

For the study of these phenomena, the mass balance was made by using theoretically calculated values and the practical values were measured by chemical analyses (Tables 2 and 4) as shown in Table 5. It was assumed that each component ratio in the produced ingot was preserved the same as that when it was charged even though the crusts contained more ZrO_2. For example, in the TROI-49 test, because the charged weight was 15.961 kg and the produced ingot weight was 10.575 kg of which the upper layer was 8.21 kg and the lower layer was 2.365 kg as shown in Fig. 3, this means that 66.26% of the charged materials were solidified as an ingot as shown in Table 5. Since each component in the ingot was assumed to solidify at the same ratio as the charged mass, 2.394 kg of the initial charged ZrO_2 would form 1.586 kg in the ingot. However, the actual produced ZrO_2 weight was 2.539 kg (1.880 kg Zr) from the calculation, where this value was obtained from a multiplication of the upper layer weight of 8.21 kg with the averaged ZrO_2 content of 30.92% for TROI-49 shown in Table 2. As shown in Table 5, the result shows that the actual produced ZrO_2 weight was 0.953 kg (7.726 g mol) more than the theoretical produced weight.

The charged zirconium metal mass was 1.867 kg, so the Zr-metal mass in the ingot would theoretically be 1.237 kg Zr, which is a multiplication of the charged mass with the solidified ratio. The actual produced zirconium metal mass was 0.666 kg Zr, which is a

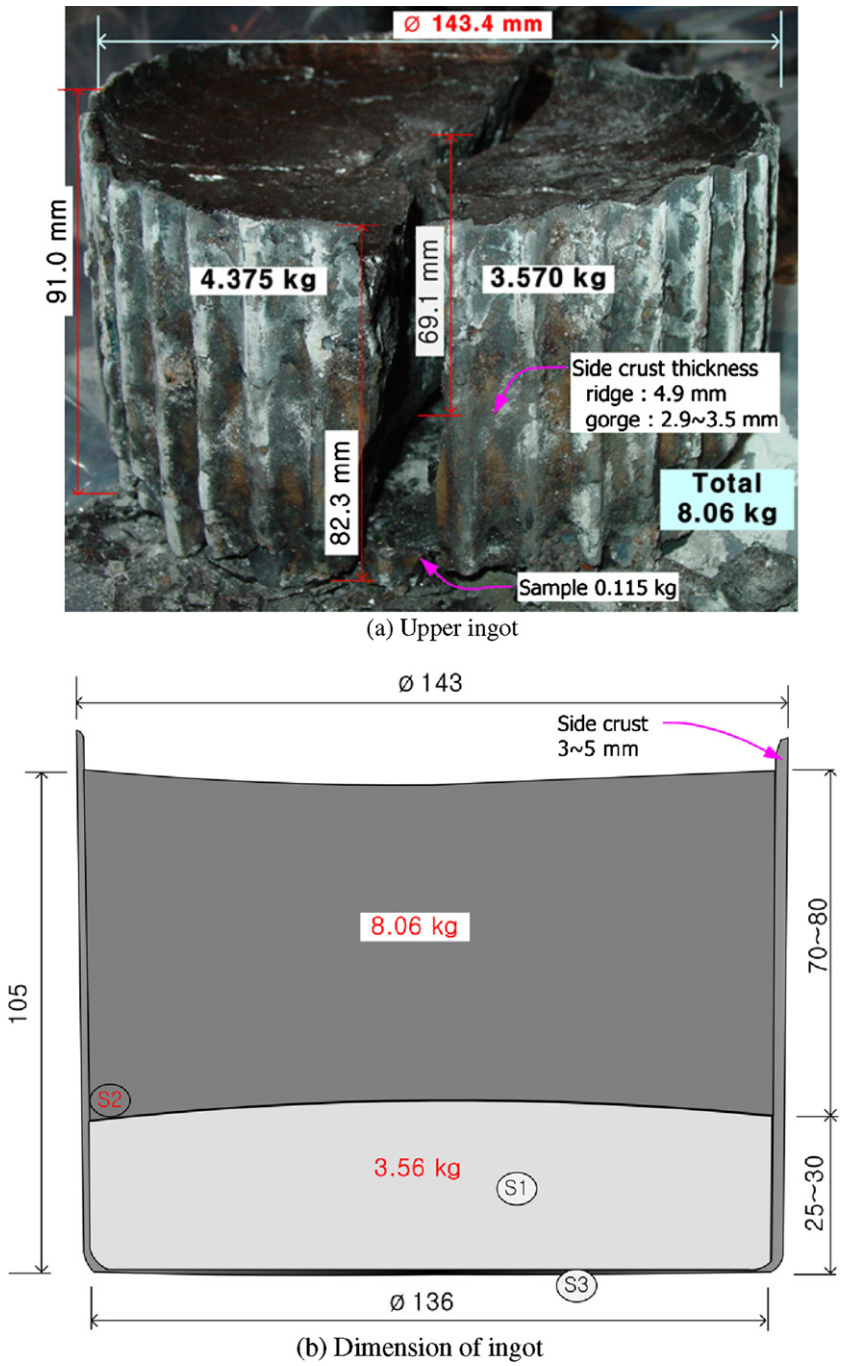

Fig. 4. Photograph of upper ingot and sketch of overall ingot (TROI-50).

Table 1
Analysis results by the ICP-AES (wt%)

		U	Zr	Fe	Cr	Ni	Sum
Upper layer, 1	#49	61.75	22.93	0.36	0.16	0.06	85.26
	#50	55.54	24.13	0.55	<100	<100	80.22
Upper layer, 2	#49	61.44	22.85	0.82	0.25	0.1	85.46
	#50	54.48	23.47	0.4	<100	<100	78.35
Lower layer	#49	33.73	20.53	30.97	6.2	2.89	94.32
	#50	31.73	16.66	48.4	0.03	0.02	96.84

Table 2
Calculation results of oxide compounds for metal components of the ICP-AES in Table 1 (wt%)

		UO_2	ZrO_2	Fe_2O_3	Cr_2O_3	NiO	Sum
Upper layer, 1	#49	70.05	30.97	0.51	0.23	0.08	101.85
	#50	63	32.6	0.79	<100	<100	96.39
Upper layer, 2	#49	69.70	30.87	1.17	0.37	0.13	102.23
	#50	61.80	31.70	0.57	<100	<100	94.07
Lower layer	#49	38.26	27.73	44.28	9.06	3.68	123.01
	#50	36.00	22.50	69.20	0.04	0.03	127.77

Table 3
Analysis results by the EPMA (wt%)

		U	Zr	Fe	Cr	Ni	O
Upper layer, 1	#49	50.47	20.83				28.7
	#50	51.00	21.20	0.54			27.3
Upper layer, 2	#49	51.87	20.77				27.37
	#50	47.90	28.20	0.28			29.6
Lower layer	#49	33.4	24.4	21.4	5.47	1.95	13.34
	#50	28.40	20.40	31.5			19.7

Table 4
Normalization results of oxides and metals after exclusion of the oxygen amount in the EPMA analysis of Table 3 (wt%)

	No.	UO_2	ZrO_2	Fe_2O_3	Cr_2O_3	NiO
Upper layer, 1	#49	67.05	32.95			
	#50	66.30	32.82	0.88		
Upper layer, 2	#49	67.71	32.29			
	#50	59.30	41.03	0.43		
		U	Zr	Fe	Cr	Ni
Lower layer	#49	38.56	28.17	24.71	6.31	2.25
	#50	35.37	25.40	39.23		

Table 5
Mass balance of charged materials and products

TROI-49		TROI-50
Charge weight	15.961 kg	14.456 kg
Produced ingot weight		
Ingot	10.575 kg	11.62 kg
Upper	8.21 kg	8.06 kg
Lower	2.365 kg	3.56 kg
Ingot ratio for charged corium mass	66.255%	80.38%
Theoretical composition distribution		
ZrO_2		
Charged	2.394 kg	2.605 kg
Ingot	1.586 kg(1.376 kg Zr)	2.094 kg (1.55 kg Zr)
Zr		
Charged	kg	1.72 kg
Ingot	1.237 kg	1.383 kg
UO_2		
Charged	9.936 kg	8.605 kg
Ingot	6.583 kg(5.8 kg U)	6.917 kg(6.1 kg U)
Produced wt. (base on analysis)		
ZrO_2 (upper ingot)	2.539 kg ZrO_2 (1.880 kg Zr)	2.591 kg ZrO_2 (1.918 kg Zr)
Zr (lower ingot)	0.666 kg Zr	0.904 kg Zr
UO_2 upper ingot	5.737 kg UO_2 (5.057 kg U)	5.029 kg UO_2 (4.433 kg U)
U lower ingot	0.912 kg U	1.259 kg U
Results (theoretical − produced)		
ZrO_2	1.586 − 2.539 = −0.953 kg (7.726 g mol)	2.094 − 2.591 = −0.497 kg (4.03 g mol)
Zr	1.237 − 0.666 = 0.571 kg (6.275 g mol)	1.383 − 0.904 = 0.479 kg (5.264 g mol)
U	0.912 kg U (3.832 g mol)	1.259 kg U (5.290 g mol)

Stainless steel excluded at the mass balance.

multiplication of the lower ingot mass with the Zr content of 28.17% shown in Table 4. Consequently, the produced zirconium metal mass was 0.571 kg (6.275 g mol) less than the theoretical value. The mass of other compounds can be calculated by the same method.

In the case of the TROI-49 experiment, 6.275 mol of zirconium metal was consumed, and 7.726 mol of ZrO_2 and 3.832 mol of U were produced by using this mass balance. The formation of U and ZrO_2 can be expressed by the following two chemical reactions:

$$UO_2 + Zr \rightarrow U + ZrO_2, \quad (1)$$

$$Zr + O_2 \rightarrow ZrO_2. \quad (2)$$

In the chemical reaction of Eq. (1), Zr of 3.832 mol would react with the same moles of UO_2, and the same moles of U and ZrO_2 would be produced. The remaining 2.443 g mol of Zr metal would react with oxygen according to Eq. (2). Though ZrO_2 would be produced by 3.832 mol by Eq. (1) and 2.443 mol by Eq. (2), 1.451 mol of ZrO_2 out of an actual total of 7.726 g mol would be errors from the chemical analysis and process losses.

Therefore, zirconium metal including an initiator is expected to be oxidized at the initial heating phase and the other Zr metal would be melted and then reduce to UO_2. Table 5 also shows the material balance in the TROI-50 test. It was calculated that 5.264 mol of Zr metal would be consumed, and 5.29 mol of U and 4.03 mol of ZrO_2 were produced. Though the moles of consumed Zr were similar to that of the produced U, ZrO_2 was produced at more than 1.234 g mol by considering this material balance. This error would also come from various process losses during a charging and product collection, and so on.

In the case of TROI-50, the total theoretical produced Zr mass was estimated as 2.933 kg Zr that was 1.55 kg Zr in a ZrO_2 form and 1.383 kg Zr as metal. However, the actual produced amount based on the chemical analysis results was 1.918 kg Zr in the upper part and 0.904 kg Zr in the lower part. Total loss amount was calculated as 2.822 kg Zr. This means that 0.111 kg Zr (1.22 g mol Zr) was lost during the process.

3.2.2.4. Reduction ratio of UO_2. When nuclear fuel is melted during a severe accident in a nuclear reactor plant, the main concern is that the molten UO_2 and Zircaloy would react and affect the RPV integrity. In the TROI-49 test, 6.583 kg (5.8 kg U) of UO_2 out of 9.936 kg in the initial charge was transferred to 5.737 kg UO_2 in the upper ingot and produced by 0.912 kg U (1.035 kg UO_2) in the lower layer as shown in Table 5. Total 5.969 kg U mass in the form of an ingot was slightly larger than the theoretically calculated one (5.8 kg U) owing to the higher portion of ZrO_2 remaining in the crusts.

0.912 kg U out of a total of 5.969 kg U was reduced to a metallic form and its reduction ratio was 15.28%. In TROI-50, uranium mass contained in the ingot was 5.692 kg U theoretically and the produced uranium was 1.259 kg U in the lower ingot, and then the reduction ratio was 22.12%. These conversion ratios are almost the same as those in the MASCA test in which UO_2 was reduced by 18% [7].

3.2.2.5. Iron analysis. Stainless steel is an internal structure of a nuclear reactor and will melt with a fuel during a severe accident. The distribution of iron, a main component of stainless steel, is one of the important issues in a severe accident. In the results of the iron analysis by ICP-AES and EPMA, the iron content for the lower ingot layer varied considerably. Though the iron content was 21.4% for TROI-49 as shown in Table 3, this was an averaged value of 15.7%, 24.8% and 23.7% for three points. The iron content in the TROI-50 test was analyzed to be a higher value in spite of its lower charging ratio than that in TROI-49. These mean that iron would form an inhomogeneous mixture and its content would vary according to the sampling locations. Therefore, the contents of uranium and zirconium also vary depending on the iron content.

In the case of the TROI-49 test, as the iron content is below 1% in the upper layer and 24.7% in the lower layer (refer to Table 4), it is judged that most of the iron was deposited in the lower layer in the form of a metal or alloy. The produced mass by a homogeneous

assumption was 48 g Fe in the upper layer from Table 1 and 584 g Fe in the lower layer from Table 4 in the case of TROI-49. 92.4% of the total iron content is contained in the lower layer. For TROI-50, it was 38 g Fe in the upper layer and 1397 g Fe in the lower layer. Therefore, 97.4% of the total iron content was contained in the lower layer. Since the iron content in the stainless steel was found to be 73.1% (Cr 18.8%, Ni 7.6% and others) by a chemical analysis, the iron mass in the ingot for TROI-49 is calculated theoretically to be 854 g. The produced iron mass was 632 g by the assumption of a homogeneous composition and the difference from the theoretically calculated mass may come from the non-homogeneous distributions of Fe. However, in the case of TROI-50, the iron mass was calculated theoretically to be 896 g but the actual produced mass was 1435 g Fe. Also, the iron distribution shows a large difference depending on the positions. As previously stated, the distribution of iron was non-homogeneous, and most of the iron in the stainless steel was transferred to the lower part of the molten corium. If iron was oxidized by oxygen in air, the oxidized iron would be reduced by Zr metal as shown in Eq. (3). Therefore, iron is believed to exist in a metal state [12].

$$2Fe_2O_3 + 3Zr = 4Fe + 3ZrO_2. \quad (3)$$

3.2.2.6. Density of the products. The upper ingot was sampled by about 100 g each at five positions and their densities were measured for the TROI-49 test. Their densities were 8.767, 8.887, 7.617, 8.787 and 8.768 g/cm^3. When a sample with the lowest density is excluded, which contains quite a few pores, the averaged density is 8.802 g/cm^3.

Since the densities of UO_2 and ZrO_2 are about 10.98 g/cm^3 and 5.8 g/cm^3, the upper layer mainly consists of 69.88% of UO_2 and 30.92% of ZrO_2 as shown in Table 2. The density of this mixture is calculated as 8.66 g/cm^3 by the following equation [13]:

$$\rho_c = \frac{0.27f(UO_2) + 0.123f(ZrO_2)}{\frac{0.27f(UO_2)}{\rho(UO_2)} + \frac{0.123f(ZrO_2)}{\rho(ZrO_2)}}, \quad (4)$$

where $f(i)$ is the atomic fraction of ith component and ρ is the density of ith component.

The density of the lower ingot was measured as 9.248, 9.358, 9.496, 9.541, 8.608 g/cm^3 for five samples of about 100–200 g. The averaged density was 9.411 g/cm^3, when a sample with the lowest density is excluded, which contained some impurities. The lower metal layer is assumed to consist of a homogeneous mixture except for iron as shown in Table 4 and considering that the density of each component is U = 19.07, Zr = 6.49, Fe = 7.86, Cr = 7.19, Ni = 8.9 g/cm^3, the averaged density of the lower part is calculated as 11.78 g/cm^3 for TROI-49 and 11.47 g/cm^3 for TROI-50. Though the measured density is lower than the theoretically calculated value, the lower layer of the ingot is thought to exist in a metal state when considering an imperfect compactness due to the fine pores.

3.2.2.7. XRD analysis. To obtain the chemical information on the two layers, the chemical compounds of the products were analyzed by XRD. The upper layer mostly consists of UO_2 as shown in Fig. 5. It shows almost consistent peak characteristics of the debris such that the UO_2 peaks were shifted because Zr atoms were inserted into the cubic UO_2 lattice [14]. In the lower layer of the ingot, most of the iron was inferred to form Fe_2U alloy as shown in Fig. 6. If this molecular ratio is applied, 428 g of iron forms an alloy with U metal and the remaining 156 g Fe could form an alloy with Zr or it could be deposited in the case of TROI-49. The TROI-50 test also revealed that more than half of the iron formed an alloy with Zr or it was deposited.

3.3. Steam explosion test

In the TROI-51 test in which the melt composition was similar to that in TROI-50, the molten corium interacted with water and then the effect of its composition was investigated on a steam explosion. The charging and melting of TROI-51 was almost the same as that of TROI-50. The compositions of the charge were 60.51%, 16.67%, 12.10% and 10.72% for UO_2, ZrO_2, Zr and SS including the ZrO_2 coating weight of 0.515 kg and their total weight was 14.22 kg. After the melt was generated in the cold crucible by induction heating, the water-cooled plug was removed by using a pneumatic cylinder, and then a cone-shaped puncher perforated the bottom crust [11]. The melt was released by gravity into the water contained in the test section. The delivered melt temperature was 2695 K which was measured with a standard pyrometer. It was measured for a very short time because its descending speed was very fast at about 6 m/s.

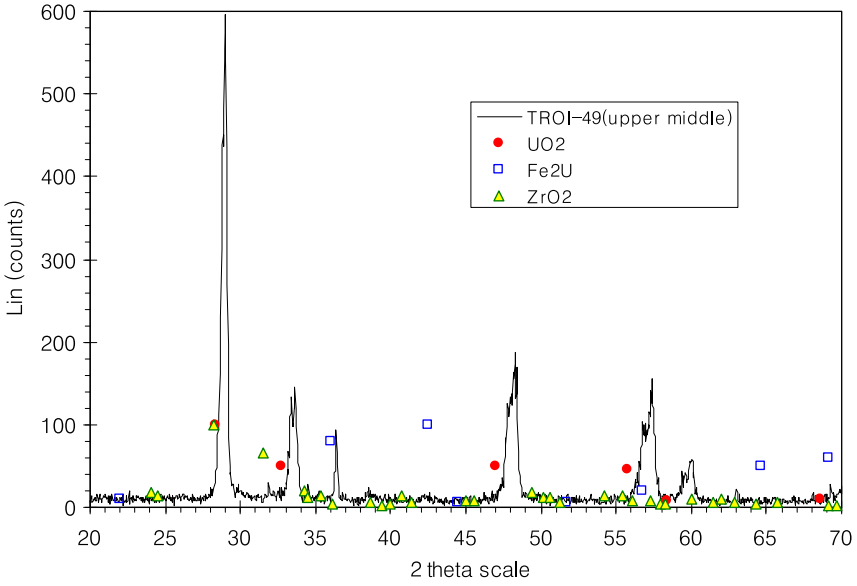

Fig. 5. XRD result for the sample from the middle of the upper layer in TROI-49.

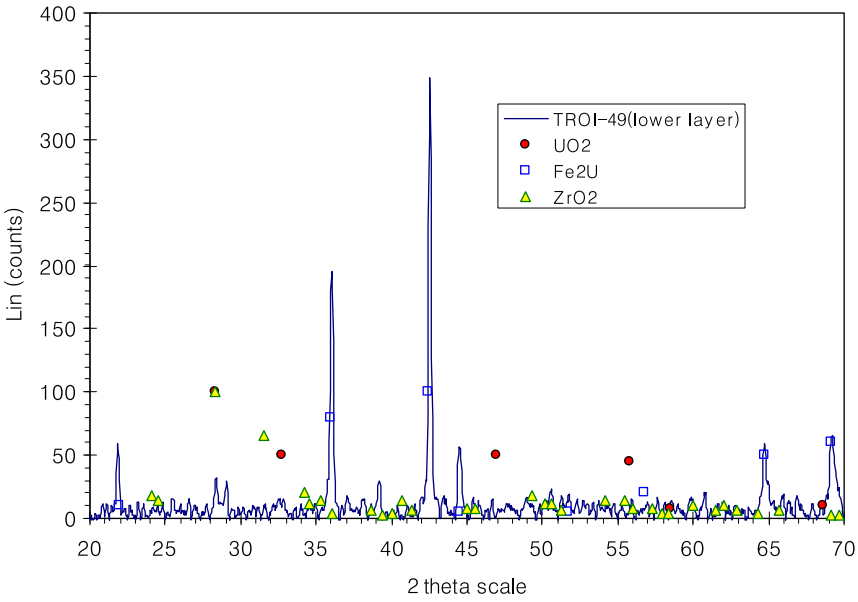

Fig. 6. XRD result for the sample from the lower layer in TROI-49.

Corium melt of 6.309 kg was poured into the water pool at a temperature of 294 K and at an ambient pressure of 0.115 MPa. Water depth was 130 cm and the water mass was 367 kg. Initial melt jet diameter was 6.5 mm. The pressure of the vessel was increased up to 0.168 MPa at 3.2 s after the melt was injected into the water. The pressure increment was 0.053 MPa [15].

The pressure peaks appearing at 1.327 s were supposed to be the peaks due to an external trigger (PETN 1.0g) and the maximum pressure was observed to be 21 MPa. The recorded maximum pressure by a steam explosion was 32 MPa. In addition, the steam explosion was initiated at 1.3285 s from the puncher actuation. The external triggering was too early for the melt to reach the bottom of the interaction vessel. The maximum value of the dynamic load on the bottom of the interaction vessel was quite high at 580 kN.

From the chemical analysis result on debris smaller than 0.425 mm, it was observed that UO_2 is 42.4%, ZrO_2 is 34.4% and Fe_2O_3 is 27%. This meant that the charged weight ratio of 78.4/21.6 of UO_2/ZrO_2 was changed to 55.2/44.8 in the debris. Since the explosive interactions for a non-eutectic composition (for example, weight ratio of UO_2/ZrO_2 = 78/22) occurred rarely, but an energetic steam explosion for an eutectic composition (UO_2/ZrO_2 = 70/30 wt%) was usually produced, this non-eutectic composition is not expected to produce a steam explosion [5,6,14]. Though it was not known from this analysis how much amounts of U and Zr metals were re-oxidized during the interaction with water, and which components contributed to the steam explosion, the metals were thought to contribute to the steam explosion.

4. Conclusions

The prototypic corium, a mixture of UO_2 pellets, ZrO_2 powder, chips of zirconium metal and stainless steel, was melted in a cold crucible by an induction heating technique under a postulated severe accident condition in a nuclear reactor. When it was melted and then solidified in the cold crucible, the molten corium was separated into two layers: an upper oxide layer and a lower metal layer.

The results of the ICP-AES, EPMA, XRD analysis and a density measurement show that the upper mixture consisted of oxides such as UO_2 and ZrO_2, and the lower layer was metals such as U, Zr and stainless steel. The uranium metal in the lower layer was produced by reduction of UO_2 by Zr metal and the oxidation ratio of UO_2 was 15.28% and 22.12% for TROI-49 and 50, respectively. The ZrO_2 was produced by oxidation of Zr metal by oxygen in the air as well as a reaction between Zr and UO_2.

The averaged density of the upper oxide layer was 8.802 g/cm^3 and that of the metal layer was 9.411 g/cm^3. Although iron, the main component of stainless steel, and zirconium have a lower density than the upper oxide layer, they were located in the lower layer as an alloy with a high density uranium metal. Iron does not form a homogeneous solution and its content varied with the positions. Iron did not reduce the UO_2 and ZrO_2 to metal and it existed as a metal and about a half of it formed an alloy as Fe_2U.

When the metal-added molten corium interacted with water, the metals such as the produced U and zirconium and the charged iron and zirconium were considered to have rapid heat transfer characteristics compared to the oxide materials and to affect the hydrogen generation by a reaction with water. The metal-added corium in this test showed a strong steam explosion in spite of its non-eutectic composition. Therefore, corium-containing metals have to be considered for a failure of a RPV by a high heat flux from phase-separated metals and for their effect on a steam explosion during a severe accident in a nuclear reactor.

Acknowledgement

This study has been carried out under the nuclear R&D program by the Korean Ministry of Science and Technology.

References

[1] J.M. Broughton, P. Kuan, D.A. Petti, E.L. Tolman, Nucl. Tech. 87 (1989) 34.
[2] L.A. Sticker, J.L. Rempe, S.A. Chavez, et al., NUREG/CR-6196 (1994) 58.
[3] D. Magallon, I. Huhtiniemi, H. Hohmann, Nucl. Eng. Des. 189 (1999) 223.
[4] D. Magallon, I. Huhtiniemi, Nucl. Eng. Des. 204 (2001) 369.
[5] I. Huhtiniemi, D. Magallon, H. Hohmann, Nucl. Eng. Des. 189 (1999) 379.
[6] I. Huhtiniemi, D. Magallon, Nucl. Eng. Des. 204 (2001) 391.
[7] S.V. Bechta, Personal Communication, Alexandrov Research Institute of Technology, Kurchatov Institute, 2006.
[8] J.H. Song, B.T. Min, et al., Heat Mass Transfer 32 (2005) 1325.
[9] J.H. Song, I.K. Park, Y.S. Shin, J.H. Kim, S.W. Hong, B.T. Min, H.D. Kim, Nucl. Eng. Des. 222 (2003) 1.
[10] S.W. Hong, B.T. Min, J.H. Song, H.D. Kim, J.K. Choi, in: Proceedings of the Second Japan–Korea Symposium on Nuclear Thermal Hydraulics and Safety, Fukuoka, Japan, 2000.

[11] B.T. Min, S.W. Hong, et al., in: Proceedings of the ICAPP'04, Pittsburgh, PA USA, June 13–17, 2004, Paper 4222, p. 1173.
[12] A.A. Sulatsky, S.V. Bechta, et al., in: Proceedings of the ICAPP 05, Seoul, Korea, May 15–19, 2005, Paper 5240.
[13] D.T. Hagrman (ed.), MATPRO: NUREG/CR-6150, SCDAP/RELAP5/MOD 3.1 Code Manual, vol. IV, 1993.
[14] J.H. Kim, I.K. Park, B.T. Min, S.W. Hong, J.H. Song, H.D. Kim, in: Proceedings of the NUTHOS-6, Nara, Japan, October 4–8, 2004.
[15] J.H. Kim, B.T. Min, S.W. Hong, et al., in: Eighteenth International Symposium on Transport Phenomena, 27–30 August, 2007, Daejeon, Korea.